

Comparison of atmospheric spectral radiance measurements from five independently calibrated systems

D. Pissulla,^{*a} G. Seckmeyer,^a R. R. Cordero,^{b,c} M. Blumthaler,^d B. Schallhart,^d A. Webb,^e R. Kift,^e A. Smedley,^e A. F. Bais,^f N. Kouremeti,^f A. Cede,^g J. Herman^g and M. Kowalewski^g

Received 30th September 2008, Accepted 26th January 2009

First published as an Advance Article on the web 9th February 2009

DOI: 10.1039/b817018e

A variety of instruments have been developed over the past 50 years to measure spectral radiance in absolute units at UV and visible wavelengths with high spectral resolution. While there is considerable experience in the measurement of spectral irradiance, less emphasis has been given to the reliable measurement of spectral radiance from ground observations. We discuss the methodology and calibration procedures for five instruments capable of making such measurements. Four of these instruments are based on double monochromators that scan each wavelength in turn, and one is based on a single monochromator with a charged coupled device (CCD) allowing the recording of all wavelengths simultaneously. The measured spectral radiance deviates between 3% and about 35% depending on the instruments. The results are compared with radiative transfer calculations when the aerosol characteristics of the atmosphere are known.

Introduction

The energy for running dynamical processes within the atmosphere and for life on Earth depends on the continual supply of the sun's radiation. This incoming energy can be described by a combination of separate spectral direct-sun and sky radiance measurements. In contrast to spectral global irradiance, which refers to the incident power on a horizontal surface,¹ spectral sky radiance provides both spectral and spatial information about the radiation field. The additional spatial and spectral information included in spectral sky radiance is essential for many applications. Improving the knowledge of sky radiance is valuable in many research areas, ranging from medical research on the impact of ultraviolet radiation on various parts of the body, to solar lighting predictions for architecture, and the development of radiation models for predicting climate change and its biological effects.

C. Dorno was the first scientist to publish radiance measurements.² In his publication he laid the foundation of radiation climatology. He determined the cause of the healing effect of the high mountain climate to be a combination of the environment and complete physical rest. Later the intensity of diffuse short-wave radiation at Davos during overcast conditions and its dependence on cloud type and solar altitude was investigated.³ He found out that for the summer period at a solar altitude of 50°

the mean intensities of diffuse radiation are 1.6 to 6.2 times greater than the clear sky values, depending on the type of cloud form. During the winter period, the intensities can be 1.15 to 1.92 times greater than the summer values. More recent measurements of spectral sky radiance have been made.⁴ Measurements at various locations throughout Europe were used to investigate the sky radiance under a selection of atmospheric conditions. These reveal variations in the spatial distribution of sky radiance in the UV-B of up to a factor of 2, and in the UV-A of up to a factor of 10 across the hemisphere. Furthermore, a distinct minimum of sky radiance, which is dependent on the solar zenith angle (SZA), but not on wavelength, was observed. Ref. 5 reports measured sky radiance at a high-latitude, coastal site under clear and cloudy conditions using an all-sky camera and a narrow field-of-view spectroradiometer. These observations were compared to results from a 3D Monte-Carlo radiation model that explicitly includes the interaction of radiation with heterogeneous surface features. The observed sky radiance distribution showed good agreement with modelled results and roughly mirrored the spatial distribution of surface albedo. A recent study⁶ describes spectral sky radiance measurements over a snow covered surface at an alpine site. A comparison of the experimental data with model results from a 1D radiative transfer model showed that for the case of homogeneously snow-covered terrain, when the snow melted the diffuse sky radiance was reduced by up to 40%, depending on solar zenith angle. In addition, it was found that diffuse sky radiance measurements in a low aerosol environment are especially useful in the assessment and validation of radiative transfer models. Spectral sky radiance measurements were made by the Institute of Meteorology and Climatology of the Leibniz Universität Hannover (DEH) in an Antarctic environment to investigate the impact of high snow albedo on spectral sky radiance.⁷⁻⁸ The measurements show that the radiance distribution over the sky becomes less homogeneous with increasing wavelength. These results were confirmed by model results. For a SZA of 86° at

^aInstitute of Meteorology and Climatology, Leibniz Universität Hannover, Germany. E-mail: Pissulla@muk.uni-hannover.de

^bUniversidad Técnica Federico Santa María, Ave. España 1680, Valparaiso, Chile

^cUniversidad de Santiago de Chile, Casilla 307 Correo 2, Santiago, Chile

^dDivision of Biomedical Physics, Innsbruck Medical University, Austria

^eSchool of Earth, Atmospheric and Environmental Sciences, University of Manchester, United Kingdom

^fLaboratory of Atmospheric Physics, Aristotle University of Thessaloniki, Greece

^gNASA/Goddard Space Flight Center, Greenbelt, Maryland, USA

Table 1 List of all instruments involved in this study

Institute/Abbreviation	Optical part of the instrument	Instrument type spectral range/nm	Radiance optics FOV/°	FWHM/nm	Calibration method
University of Hannover/DEH	Bentham TMc 300	280 to 2500	4.5	0.5 to 10	Lamp + diffuser plate
Innsbruck/ATI	Bentham DTM 300	280 to 600	1.4	0.52	Integrating sphere Direct irradiance calibration + geometrical factor
University of Manchester/GBM	Bentham DTM 300	280 to 600	1.0	0.6	
Aristotle University of Thessaloniki/GRT	Single monochromator with CCD	310 to 1000	3.6	1.8 (UV-B) to 2.65 (VIS)	Lamp + diffuser plate
NASA/Goddard Space Flight Center/USB	Brewer MKIII	283 to 364	0.5	0.47 to 0.67	Lamp + diffuser plate, integrating sphere

a wavelength of 305 nm, the sky radiance at the horizon was only about 80% of the zenith sky radiance. But at 1000 nm, the measured sky radiance at the antisolar point exceeded the zenith sky radiance by a factor of 11. The difference in homogeneity at shorter wavelengths is mainly due to Rayleigh scattering, which increases at shorter wavelengths.

In this paper we describe the configurations and calibration methods for 5 instruments (listed in Table 1) and how the difference between the measurement results affects the measured sky radiance distribution. The field of view (FOV) of the radiance input optics is defined as the maximum area in degrees that can be seen through the optics.

Instruments and methods

DEH (Institute of Meteorology and Climatology, Leibniz Universität Hannover, Germany)

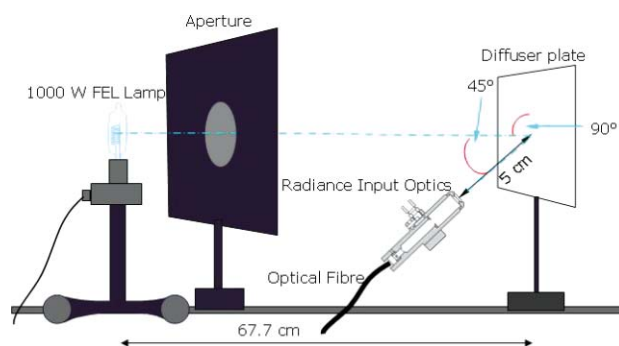
The central element of the DEH spectroradiometer is a TMc300 double monochromator manufactured by Bentham Instruments Ltd. The double monochromator consists of two identical single Czerny-Turner monochromators. The total focal length is 600 mm. The radiation enters the monochromator through a motorised entrance slit, which is set to 0.74 mm for wavelengths between 290 and 600 nm. This is also the width of the exit slit. The middle slit is set to 1.85 mm. For the wavelength range of 290 to 600 nm a holographic reflection grating with 2400 rules/mm is employed to disperse the radiation into its spectral components in each monochromator. Stray light is suppressed by a number of baffles and the middle slit. The nominal bandwidth of the spectroradiometer of the described setup is 0.5 nm.⁹

A photomultiplier (PMT), model DH-3(Bi), is employed as a detector for the wavelength range from 290 to 600 nm. To operate the spectroradiometer in a stable manner, it is placed inside a temperature controlled box. The temperature inside this weather-proof box is held at 20 °C (± 0.5 °C) during the measurements. Radiometric stability and wavelength accuracy are frequently tested.⁷ Absolute calibrations of the instrument are performed with a 1000 W FEL lamp at the DEH's radiation laboratory. The responsivity of the spectroradiometer in the field is determined by scanning a 100 W tungsten halogen lamp, which is operated inside a portable field calibrator.¹⁰ The spectral irradiance measured by this instrument has been intercompared with other spectroradiometers from New Zealand and the US.⁹

A skyscanner is used for pointing the radiance input optics at selected points in the sky and is usually used to measure the sky luminance at 145 standardised points. The mechanical control of the skyscanner is based on three electric motors driving one vertical and two horizontal axes. The vertical axis' movement is limited to 190°. This axis turns the whole body of the skyscanner. The first horizontal axis actuates the luminance detector. The second horizontal axis drives the input optics for radiance. It is limited to $\pm 90^\circ$, if 0° is set to a SZA of 0°. The whole body is mounted on a 50 cm high pedestal. An internal PC inside the skyscanner controls the motors, heating, cooling, and the luminance detector. An external PC connected *via* a serial port to the skyscanner contains the user interface and control software. To measure sky radiance, the input optics has to be mounted to the secondary horizontal axis, which is located at the bottom of the skyscanner body. At the rear end of the input optics an optical fibre has to be attached to direct the radiation to the spectroradiometer.

The input optics designed for spectral sky radiance measurements consists of a 130 mm long collimator tube that has an internal black matt-finish to avoid reflections. A baffle in the middle of the tube is used to limit the FOV and to reject stray light. The edges of the FOV cut off sharply and no local maxima can be detected. The FOV is approximately 4.5° , giving a solid angle for the input optics of 4.84×10^{-3} sr. The radiance calibration procedure is adapted from¹¹ for use in the DEH radiation laboratory facilities.

Fig. 1 shows the setup for the spectral radiance calibration. The calibrated 1000 W FEL lamp is placed in the lamp room at a specified distance from the surface of the diffuser plate. The distance was chosen to be the same as that used during the calibration procedure at Physikalisch-Technische-Bundesanstalt (PTB), namely 67.7 cm. This avoids the uncertainties introduced by applying the inverse square law to recalculate the irradiance of the measured lamp.¹² A wall between the lamp room and the laboratory acts as a baffle. The diffuser plate is made of an optically diffuse material (OP.DI.MA.). This material has a diffuse reflectance of >98% from 400 to 1600 nm and >95% from 250 to 2000 nm. OP.DI.MA. provides a uniform reflectance across this spectral range and over a large area. Other material features include long-term ultraviolet stability, high maximum permissible radiation flux densities, and the ability to be cleaned and resurfaced. The DEH diffuser plate was calibrated by Gigahertz-Optik GmbH. It is placed on an adjustable table, where a He-Ne laser is used to align the plaque perpendicular to the light beam. The radiance input optics is mounted on a rotational table at a 45° angle to the diffuser plate at a distance of about



$$D(\lambda) = \frac{S(\lambda)}{L(\lambda)} \quad (2)$$

Fig. 1 Radiance calibration setup at the DEH radiation laboratory. The radiation beam of a 1000 W FEL lamp perpendicularly illuminates the diffuser plate. The plate serves as a uniform radiation source, which illuminates the radiance input optics. The tube is placed 5 cm away in a 45° angle from the plate.

Using the spectral radiance responsivity $D(\lambda)$ and eqn (2), the spectral sky radiance $L(\lambda)$ can be calculated from the measured signal $S(\lambda)$.

5 cm. It is most important that the FOV of the collimator tube is filled by reflection from the plaque. If the tube is too far away, the input optic FOV is not uniformly illuminated by the plate and the calibration procedure is invalid.

As soon as the radiance calibration is completed a measurement of the output of a 100 W lamp within a portable calibrator is performed. This procedure is needed order to check on potential changes in the calibrations due to disassembly, moving and reassembly of the spectrometer in the field. The portable calibrator consists of an interchangeable 100 W lamp in an enclosed box with fittings that uniquely align each optical head such that the optics always views the lamps in exactly the same way. The lamp in the unit is measured immediately after calibration, and then again after reassembly at a new location, where they can also be used to track the stability of the instrument. If a full calibration is required the instrument must be removed to a laboratory.

The diffuser plate presents a uniform radiance source to the collimator tube. This arrangement avoids a partial shading of the diffuser plate by the tube or the optical fibre. To convert the measured signal to spectral radiance the radiance $L(\lambda)$ is calculated by applying the following equation.¹³

ATI (Division of Biomedical Physics, Innsbruck Medical University, Austria)

$$L(\lambda) = \frac{R(0^\circ/45^\circ, \lambda)}{\pi} \left(\frac{r_{\text{ref}}}{r} \right)^2 E(\lambda, r_{\text{ref}}) \quad (1)$$

The spectroradiometer used to measure global irradiance and actinic flux, as well as direct irradiance and radiance, consists of a double monochromator DTM300 supplied by Bentham Instruments. The focal length of each monochromator is 300 mm and both monochromators are equipped with two holographic gratings (1200 and 2400 rules/mm, respectively), that can be chosen by software. With the 1200 rules/mm grating, which is used for measurements of global irradiance and actinic flux, the slit width (FWHM) is 0.96 nm and the wavelength uncertainty is less than 0.1 nm. The input optics for the measurement of direct irradiance and radiance are connected to the second entrance slit via a Y-shaped optical fibre bundle. To obtain a better resolution at short wavelengths a 2400 rules/mm grating is used, resulting in a FWHM of about 0.52 nm and a wavelength uncertainty of less than 0.05 nm, for this kind of measurement.

where $R(0^\circ/45^\circ, \lambda)$ is the directional/directional reflectance factor of the diffuser plate, r is the measured distance between the lamp and the plate in cm, and E is the spectral irradiance of the calibrated lamp at the reference distance $r_{\text{ref}} = 67.7$ cm, interpolated to the designated λ . The interpolation is needed since PTB provided the lamp certificate in 10 to 50 nm steps only. The reflectance factor $R(0^\circ/45^\circ, \lambda)$ reflects the fact that the direct beam perpendicularly illuminates the diffuser plate (0°) and the reflected radiation is measured at an angle of 45° to the plate. For the values of the reflectance factor R the 8° /hemispherical reflectance function, $R(8^\circ/h, \lambda)$, has been used. The directional-hemispherical reflectance (here: 8° /hemispherical) is defined as reflectance, where the incident radiance is confined (in a narrow range) to a single direction (here: 8°) and the reflected radiance is collected over the complete hemisphere above the surface.¹⁴ The values of the reflectance function have been provided by Gigahertz-Optik for the DEH plate at the time of purchase. The provided reflectance values are not suitable for DEH's setup $R(0^\circ/45^\circ, \lambda)$ since Gigahertz-Optik was not able to perform calibrations in the $R(0^\circ/45^\circ, \lambda)$ direction. Johnson *et al.* give a possible additional uncertainty of 2% between $R(0^\circ/45^\circ, \lambda)$ and $R(8^\circ/h, \lambda)$.¹³ At present there is no better information on how to estimate this contribution. Previous experience^{12,15-16} in dealing with the uncertainty analysis of absolute radiation measurements suggest more work is needed before this can be put on a more rigorous basis.

To enable the spectrometer to be stable whilst being used in measurement campaigns all over Europe in a large range of weather and temperature conditions, the instrument is placed together with other sensitive hardware in an insulated box that is temperature stabilized at 28.5 °C by Peltier elements. Moreover a second weather proof box protects the instrument against snow and rain.

With $L(\lambda)$, and the measured signal $S(\lambda)$ of a known radiance source, the spectral radiance responsivity $D(\lambda)$ can be calculated with the following equation:

The sun tracking system with input optics for the measurement of direct irradiance and radiance is custom-made. It consists of two micro-stepping motors with a resolution of 0.025°. The accuracy of the position of the optics in the sky has been determined to 0.05° by using optical encoders in a feed-back loop. The Y-shaped optical fibre bundle that connects both input optics with the spectroradiometer is split at a ratio of 1 : 9. By connecting the small bundle to the direct input optics the high radiance of the solar radiation coming directly from the sun is scaled down by a factor of 9 to avoid saturation of the photomultiplier. In addition a grounded quartz plate inside the optic also reduces the intensity. Baffles are used that give a field of view of about 1.5° for these input optics.

The input optics for the measurement of radiance consists of a lens above an aperture, a linear polarizing filter and the shutter

above the entrance of the thicker fibre bundle. In addition a tube with baffles in front of the lens reduces stray light. The lens with a focal length of 10 cm focuses the light from the sky onto the aperture which gives a field of view of 1.4° , so that the solid angle is 4.69×10^{-4} sr. The spectral transmittance of the polarizing filter is shown in Fig. 2.

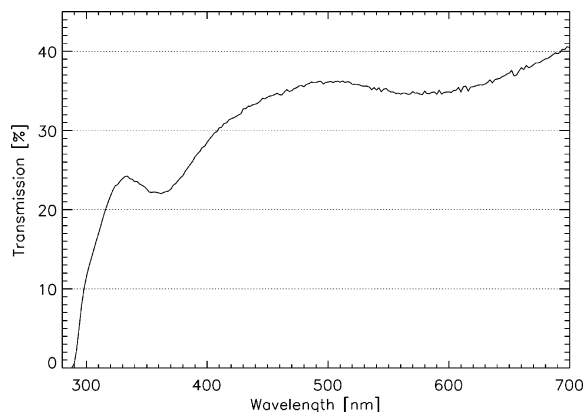


Fig. 2 Transmission of the linear polarizing filter inside the radiance input optic.

It is usual for the polarizing filter to be mounted in the radiance input optics. Especially during calibration, this allows the spectral behaviour of the filter to be accounted for. Moreover the alignment of the transmission axis of the polarizing filter can be chosen by the software, when sky scans are performed and radiation from selected positions in the sky is measured at a chosen wavelength. At each position four measurements with different orientations (0° , 45° , 90° and 135°) of the transmission axis of the polarizing filter are performed. This information is then used to calculate the degree and angle of polarization by means of the Stokes parameters at each position. The unpolarised radiance can be obtained by adding the polarized radiances gained at crossed orientations (0° and 90° , or alternatively 45° and 135°) of the transmission axis of the polarizing filter. The two possible results for unpolarised radiance match at a 99% level. Moreover full spectra of polarized radiance can be obtained with a predefined orientation of the transmission axis of the polarizing filter.

The calibration of the radiance input optic is based on an integrating sphere, which is calibrated by Gigahertz Optik GmbH and traceable to PTB. The uncertainty of the certificate of the sphere in the wavelengths range 270 to 395 nm is given as $\pm 6\%$ ($k = 2$) and from 400 to 780 nm it is determined to be $\pm 5\%$ ($k = 2$). The sphere with a diameter of 15 cm is laminated with totally diffuse reflecting OP.DI.MA. A 100 W halogen lamp is mounted at the input port of the sphere. At the 2.5 cm diameter output port diffuse light exits the sphere, which is measured with the radiance input optics for absolute calibration. Then the certificate of the sphere is transferred to the portable field calibrator, which is used for routine calibration. Earlier a diffuser plate at a distance of 70 cm from the 1000 W lamp was used for calibration. This kind of setup was found to be very sensitive to stray light and had very low signal at wavelengths below 350 nm, therefore the diffuser plate is no longer in use.

Measurements of global irradiance, actinic flux and direct irradiance accomplished with this spectroradiometer have already

been compared to other instruments at diverse European campaigns. See ref. 17–19 for more details.

GBM (School of Earth Atmospheric and Environmental Sciences, University of Manchester, United Kingdom)

The radiance measurements of the University of Manchester were made using a Bentham DTM300 spectroradiometer. This is similar in design to the Bentham described above operated by ATI with a FWHM of 0.6 nm. The instrument is calibrated and operated in a temperature stabilised box at $25^\circ\text{C} \pm 0.5$. The Bentham GBM has two switchable inputs to allow a variety of measurements depending on the input optics fitted. For the only campaign in this paper in which Manchester made radiance measurements (at Izaña) a head to measure global irradiance was fitted to one entrance. Whilst for the second entrance aperture a 5 m quartz fibre is fitted to a tubular input optic containing lenses and baffles with a 1° FOV. This input optic can be used for both direct (when fitted with a quartz filter to reduce the solar radiation) and radiance measurements.

The Manchester sun-tracker is a custom designed system contained within a weatherproof box, mounted atop a tripod. Inside the weatherproof box, two stepper motors, *via* 1 : 50 gearing mechanisms, control the azimuth and elevation rotations, with a single step equating to 0.03° . Microswitches prevent rotation beyond $\sim 30^\circ$ below the horizon, or past North in either direction. Full access, however, is provided to all directions in the upper hemisphere.

The setup for calibration was performed in a darkroom using a NIST traceable 1000 W lamp. The global head was calibrated using the standard methodology. The direct calibration was performed at a distance of 4.5 m in the lab to keep signal levels from saturating the Bentham PMT. The lamp was centred in the FOV of the telescope used to make the direct and radiance measurements. The calibration file obtained had to be corrected using the inverse square law to allow for the non-standard calibration distance. The calibration was performed for the spectral range of 290 to 600 nm. Finally for radiance measurements the calibration was obtained from the direct calibration by use of a geometrical factor to correct for the FOV.

As soon as each calibration is completed a measurement is made of the output from two 200 W lamps. These are then used as a transfer standard to check on changes in the calibrations due to disassembly, moving and reassembly of the spectrometer in the field. For further details about this approach see the DEH subsection in the “Instruments and methods” section.

GRT (Laboratory of Atmospheric Physics, University of Thessaloniki, Greece)

The GRT spectrograph measures direct solar irradiance and sky radiance from 310 to 1000 nm in 1000 spectral bins. This results in an average wavelength interval of 0.77 nm, ranging from 0.8 nm in the UV to 0.74 nm in the near IR region. The detector of the spectrograph is a solid state CCD (Charged Coupled Device) type S7031 by Hamamatsu Photonics. Two telescopes are used to collect the incoming radiation and are connected with the spectrograph through a UV enhanced optical fibre. The optical telescopes consist of two parallel aluminium tubes which are filled

with cylindrical baffles of different apertures. The field of view (FOV) is set to 1.2° for the direct irradiance and to 3.6° for the sky radiance optics. Depending on the application, both FOVs can be adjusted by changing the baffles inside the tubes. The radiation passes through an entrance slit (20 μm width) and is dispersed by a flat field diffraction grating (248 lines/mm), blazed at 400 nm.

The calibration of the sky radiance is performed with the use of a 1000 W DXW calibration lamp and a standard diffuser plate (OP.DI.MA) calibrated by Gigahertz-Optik GmbH. The diffuser plate is set at a distance of 50 cm from the lamp and the telescope of the radiance optics was aligned to viewing the plate at an angle of about 5° from the normal on the centre of the plate. The telescope was positioned behind the lamp, in such a way that the lamp was completely outside of its field of view. The reflectivity of a diffuser plate can be described through the following quantities:²⁰ the bidirectional reflectance distribution function (BRDF) f_r , the bidirectional reflectance factor (BRF) R and the hemispherical reflection factor ρ . For a perfectly Lambertian surface, f_r is 1/π sr⁻¹ while R and ρ are equal to unity. The calibration certificate of the diffuser plate used in this study provides the hemispherical reflection factor, ρ :

$$\rho(\theta_i, \phi_i; \lambda) = \frac{1}{\pi} \int_{\phi_r=0}^{\phi_r=2\pi} \int_{\theta_r=0}^{\theta_r=\frac{\pi}{2}} R(\theta_i, \phi_i; \theta_r, \phi_r; \lambda) \cos(\theta_r) \sin(\theta_r) d\theta_r d\phi_r \quad (3)$$

where θ_i and ϕ_i are the zenith and azimuth angles of incidence irradiance, respectively, and θ_r and ϕ_r the corresponding zenith and azimuth viewing angles of the diffuser surface, while R is unknown. Assuming that the diffuser plate behaves as a Lambertian surface, the radiance $L(\lambda)$ emitted by the diffuser plate is given by eqn (1) where both r and r_{ref} equal 50 cm and $R(0^\circ/45^\circ, \lambda)$ is substituted by $R(0^\circ/5^\circ, \lambda)$. The error introduced by the assumption that $R(0^\circ/5^\circ, \lambda)$ equals $R(8^\circ/h, \lambda)$ can be up to 5%.²¹ Finally, the distance of the telescope from the diffuser plate is not essential, as long as the plate overfills the field of view of the entrance optics. The response function for an integration time IT and wavelength λ is calculated from the following equation:

$$R(\lambda, IT) = \left(\frac{IT}{IT_{\text{ref}}} \right) \frac{L(\lambda)}{S^c(\lambda, IT_{\text{ref}})} \quad (4)$$

where $S^c(\lambda, IT_{\text{ref}})$ is the dark current and stray light corrected measurement performed using integration time IT_{ref} . IT_{ref} is the maximum integration time in order to avoid saturation of the detector.

USB (NASA/Goddard Space Flight Center, Greenbelt, Maryland, USA)

Direct irradiance and sky radiance were measured with a modified Brewer MKIII grating double spectrometer.²² The instrument contains two modified Ebert $f/6$ spectrometers with focal length 16 cm, each utilizing 3600 lines per mm holographic diffraction gratings operated in the first order. The photosensitive element is a photomultiplier tube operating in photon counting mode. By means of a filterwheel with different neutral density filters, the count rate can be adjusted to typically 5 to 15 × 10⁵ counts per second. The instrument is heated to 20 °C, so the operating temperature range is from 20 °C to more than 40 °C. The measured

raw counts are corrected for dark count, dead time, neutral density attenuation, temperature dependence and converted into count rates.

The wavelength range of this Brewer is 282.6 to 363.6 nm and the slit function is approximately triangular with FWHM from 0.47 to 0.67 nm that decreases with increasing wavelength.²³ Internal stray light is below 10⁻⁶ W m⁻² nm⁻¹. The wavelength calibration of the instrument is done in the laboratory.²⁴ The positioning of the gratings can be reset by scanning the output of an internal mercury lamp. When applying this grating-reset-routine a few times (3 to 4) during the day, the 1-sigma wavelength uncertainty in field conditions is less than 0.01 nm.²³

The field of view is circular ~2.7° FWHM (1.7 × 10⁻³ sr) for direct sun measurements and rectangular ~0.5° × 0.05° (1.9 × 10⁻⁶ sr) for sky radiance measurements.²⁵ The resolution of the sun tracking system is 0.13° in zenith and 0.03° in azimuth. The correct tracking is checked at every direct sun measurement by comparing the calculated solar position with the actual solar position. The actual solar position is determined by moving the instrument to the position of maximum intensity.

Since the Brewer in its original design is sensitive to polarization,²⁶ a depolarizer was placed in the fore-optics and the flat quartz entrance window was replaced by a curved one.²⁷ After these modifications the residual polarization is less than 1.5% for all wavelengths.

The absolute radiometric calibration of the Brewer MKIII is done in the laboratory using 1000 W tungsten quartz-halogen primary standard lamps from NIST.²⁸ For radiance calibration USB uses both a lamp-diffuser-plate technique and an integrating sphere technique in a similar way to that described earlier in this paper. For the diffuser-plate method a Spectralon diffuser plate is placed at a distance of 50 cm from the lamp and the instrument's viewing optics point to the centre of the diffuser plate at a distance of 80 cm at an angle of 30°. The bidirectional reflectance distribution function of the diffuser plate for this angle was measured as a function of wavelength using a scatterometer.²⁹ The integrating sphere used for the other calibration method has 50 cm diameter, a 20 cm diameter port, is coated with barium sulfate and illuminated by 4 internal tungsten quartz-halogen lamps of 150 W each. Its absolute calibration is traceable to NIST irradiance standards.³⁰ The 1-sigma uncertainty above 305 nm is about 3%.

Measurement sites

Izaña

From 3 June to 13 June 2005 a spectral sky radiance intercomparison took place, alongside the better understood global spectral irradiance, and direct spectral irradiance intercomparisons. To our knowledge this was the first intercomparison of this kind worldwide. The location was the Observatorio Atmosférico de Izaña (28.3° N, 16.5° W, 2367 m above sea level) on the Canary island of Tenerife, Spain. This specific location was chosen for two reasons: Firstly, its height—only natural aerosols in the free troposphere and stratosphere or high clouds would influence the measurements. At this location aerosols often originate as dust transported from the Sahara desert in Africa which is about 300 km away in a westerly direction. The local wind field is

dominated by north-westerly winds. Secondly, the clean air—the observatory is located in the middle of the island on a mountain range, where almost no anthropogenic pollution can be observed. Therefore, this site provides very good conditions for assessing the quality of spectral measurements. A predominant meteorological attribute of the Canary Islands region is the presence of the trade wind inversion that persists throughout most of the year and is well below the altitude of the station.¹⁹

Thessaloniki

The main aim of the campaign was to quantify the effects of aerosols on surface UV radiation for different radiation quantities such as global and direct irradiance, actinic flux density, and spectral radiance as a function of zenith and azimuth angle. It was aimed at determining the optical properties of aerosols, in particular the spectral aerosol optical depth and the aerosol single scattering albedo by comparing the results with those from radiative transfer modelling. The campaign site was the roof of the Laboratory for Atmospheric Physics, Aristotle University Thessaloniki (40.4° N, 22.57° E, 60 m asl), Greece from 12 July 2006 until 25 July 2006.

Innsbruck

During the measurement campaign in Thessaloniki discrepancies between measurements of zenith radiance performed by ATI and GRT of about 20% have been found. Therefore, both groups met in the laboratory at Innsbruck (47.3° N, 11.4° E, 570 m asl) on 18 and 19 April 2007 to compare their calibration procedures.

Comparison procedure

During the campaigns the schedule was to measure spectral sky radiance in the range of 290–450 nm or up to the maximum wavelength of the particular instrument at intervals of 0.5 nm. During the Izaña campaign radiance was measured for predefined directions of the sky (see Table 3) and in Thessaloniki radiance was measured from the zenith. The measurement at each wavelength setting was time-synchronised to minimize variability induced by changes in SZA or variations in atmospheric conditions.

In Izaña and Thessaloniki the spectra measured by each instrument were converted to 2 nm resolution by the SHICRivm software package³¹ since the GRT instrument has a FWHM of 1.8 to 2.65 nm. The same SHICRivm software package was used to align all measured spectra to Fraunhofer lines which are unique absorption features of the sun's photosphere. This methodology reduced considerably the systematic wavelength structure that is otherwise observed in spectral ratios of spectra measured by spectroradiometers that have different resolutions. The same

Table 2 Atmospheric parameters (mean values) from various sites where outdoor instrument comparisons have been conducted

Site	Date	Pressure/mbar	O ₃ [DU]	AOD 340
Izaña	06.06.2005	770	290	0.132
Thessaloniki	14.07.2006	1014	318	0.62
Thessaloniki	23.07.2006	1014	297	0.47
Thessaloniki	24.07.2006	1015	306	0.66

Table 3 Scanning schedule for the spectral radiance measurements. The predefined times and the SZA, the solar azimuth angle (SAA), the viewing zenith angle (VZA), the viewing azimuth angle (VAA), and the difference between VAA and SAA for the specified relative azimuth position to the sun. The radiance input optics had to be pointed at the given VZA and VAA with respect to time to perform synchronised sky radiance measurements

Starting time [UTC]	SZA/°	SAA/°	VZA/°	VAA/°	VAA – SAA/°
08:00	67	75	0	77	2
08:30	61	78	0	77	–1
09:00	54	80	51	262	182
09:30	48	83	51	262	179
10:00	41	86	39	178	92
10:30	35	90	39	178	88
11:00	28	94	0	96	2
11:30	22	99	0	96	–3
12:00	15	107	13	295	188
12:30	9	123	13	295	172
13:00	5	169	45	290	121
13:30	7	227	45	290	63

procedure also normalized the measured spectra to a common wavelength scale.

Results

Spectral sky radiance measurements from Izaña

Spectral sky radiance was measured between 08:00 and 13:30 UTC. Spectra were taken half-hourly in the directions listed in Table 3, so measurements in the same sun relative direction were taken half an hour apart before moving to the next sun relative position. The directions were chosen to measure both forward and backward scattered radiation and radiation scattered perpendicular to the sun. Fig. 3 illustrates those spectral sky radiance measurement of DEH in $\text{Wm}^{-2} \text{sr}^{-1} \text{nm}^{-1}$ versus wavelength in nm. The colours represent measurements conducted at different SZA and refer to the beginning of each spectral scan Spectra from 08:00 and 09:00 UTC are missing on this figure due to data acquisition problems.

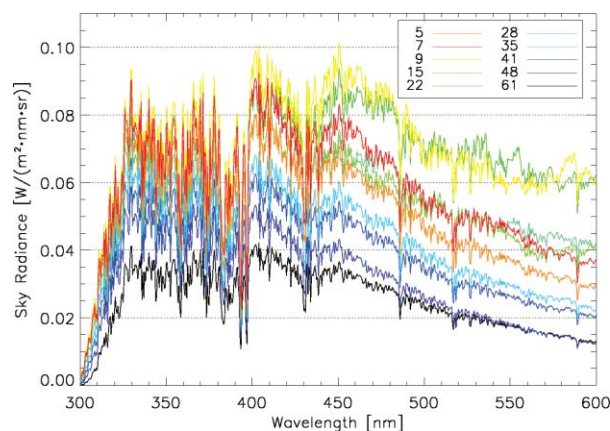


Fig. 3 Spectral sky radiance spectra from DEH measured half-hourly in Izaña on 6th of June, 2005. The spectra were taken in directional pairs half an hour apart. The details are listed in Table 3.

The spectral sky radiance increases between 290 and 330 nm, as a result of decreasing ozone absorption, remains constant until a

wavelength of approximately 450 nm, and from there on it slowly decreases. This pattern occurs in all measurements and therefore it is independent of the viewing direction. The spectrum taken at a SZA of 61° shows the lowest spectral sky radiance of all with a maximum of $0.04 \text{ W m}^{-2} \text{ sr}^{-1} \text{ nm}^{-1}$ at 400 nm. Considering this high SZA, this is not surprising. The highest values of spectral sky radiance, $0.1 \text{ W m}^{-2} \text{ sr}^{-1} \text{ nm}^{-1}$ at both 400 and 450 nm, can be found on the spectrum taken at a SZA of 9°.

In the case of the presented sky radiance measurements in Fig. 3, only scattered radiation has been measured. Thus, the measured values depend on the interplay between the amount of incoming solar radiation, which is scattered, and the wavelength depended Rayleigh function (λ^{-4} with λ being the wavelength), which causes the scattering. For the wavelength range between 330 and 450 nm the extraterrestrial irradiance radiation to be scattered increases with increasing wavelength. In contrast, the scattering caused by Rayleigh scattering decreases with increasing wavelength. The combined effect leads to the almost constant values for sky radiance between 330 and 450 nm. For wavelengths longer than 450 nm both the relative contribution of Rayleigh scattering and the extraterrestrial irradiance decrease, resulting in the drop-off of spectral radiance. Fig. 4 shows ratios of the described radiance measurements to the extraterrestrial spectrum in arbitrary units to better reflect this paragraph.

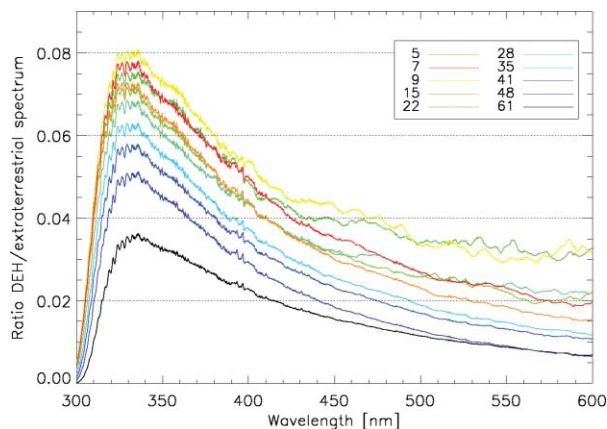


Fig. 4 Ratios of measured radiance to the extraterrestrial spectrum in arbitrary units. The evidence of amplifying Rayleigh scattering with decreased wavelength is proved by the increasing ratios.

Fig. 5 shows the ratio of spectral sky radiance measurements of ATI, GBM, and GRT over DEH performed on 6 June 2005 at 3 selected wavelength bands. The last measurement was performed at 13:30 UTC, and therefore results from the afternoon are missing.

It can be recognized that the ratio of ATI to DEH remains about 1.1 throughout the entire measurement period. It can be concluded that a wider FOV of the input optics will not have a great impact on the measurements if the direction of the measurements is sufficiently far from the direction of the Sun. ATI has a much narrower FOV (1.4°) compared to 4.5° of DEH.

The comparison of GBM to DEH is very similar to the one of ATI/DEH, but with slightly larger wavelength dependence. The respective ratios are between 0.98 and 1.1 throughout the measurement period.

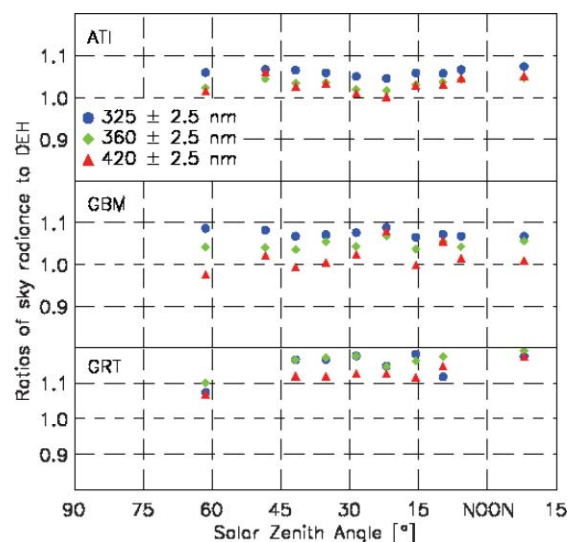


Fig. 5 Comparison of measured spectral sky radiance of ATI, GBM, and GRT to DEH measurement results in Izaña. The ratios of ATI to DEH and GBM to DEH are between unity and 1.1. The ratio of GRT data to DEH data is more than 10% higher than unity, which indicates a systematic measurement difference in one or all instruments.

In contrast, the spread of the ratios GRT to DEH during each measurement is higher with up to 20% difference for $+8^\circ$ SZA. Nonetheless, the wavelength dependence is similar to the other two instruments, but the ratios GRT/DEH are about 10% higher. The large deviation indicates a possible calibration problem with the GRT instrument since the spectral sky radiance measured by ATI and GBM is closer to DEH. However, it should be noted that the other instruments are Bentham spectroradiometers, whereas the GRT instrument is a CCD spectrograph. Therefore the difference could be also due to another unexplained systematic effect.

Fig. 6 presents spectral ratios of sky radiance measurements conducted by DEH on 6 June 2005 to model calculations of UVSPEC.³² The SZAs can be found in the legend with the corresponding colours of the ratios. The aerosol input parameters (Ångström's α and β) for the model were measured on

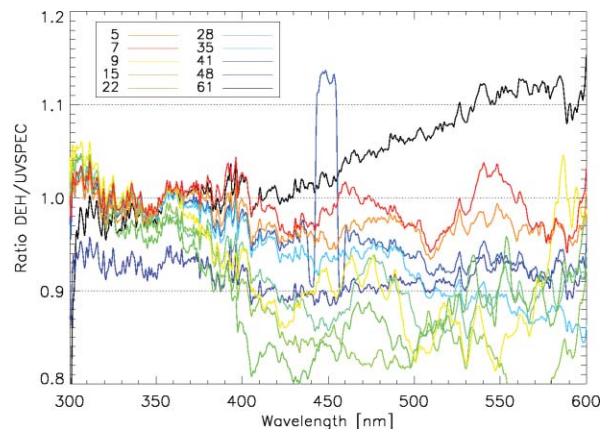


Fig. 6 Spectral ratios of DEH sky radiance measurements from day 6 June 2005 to UVSPEC modelled values. Numbers on the right denote the different solar zenith angles.

site by means of a Cimel sun photometer which is part of Aeronet.³³

The agreement between model calculations and measurements ranges from 0.9 to 1.05 for wavelengths between 305 and 390 nm. For wavelengths longer than 390 nm the ratio of the 61° SZA comparison increases up to 1.15 whereas all other ratios remain nearly constant or decrease with increasing wavelength down to 0.8. This decrease is independent of either measurement date or VZA and VAA. A single outlier occurs between 440 and 460 nm for the 41° SZA comparison. Since the intercomparison with other instruments gave no indication of an instrumental problem, it is likely that the atmospheric conditions changed rapidly (passage of a small cloud or similar) during the measurement between 440 and 460 nm which could not be reflected in the model data.

Polarised spectral sky radiance from Izaña

The radiance at the zenith was measured by rotating the input optics 360° in azimuth. This allows a check of the sensitivity of the instruments to polarization, as radiation from the zenith is polarized. Then using the filters in the ATI instrument an additional measurement of the zenith radiance was made. This was achieved using crossed orientations of the transmission axis of the polarizing filter (see ATI subsection in the “Instruments and methods” section for further details).

Fig. 7 shows the relative changes of the spectral radiance at different azimuths for the mean of all measurements. To account for slight changes in the zenith radiation during the scanning time of about two minutes, the first and the last point of the measurements was taken at the same azimuth and all measurements were corrected by linear interpolation. All instruments were proved to be almost insensitive to polarized zenith radiance with deviations of less than ±2%, which is within the measurement uncertainty.

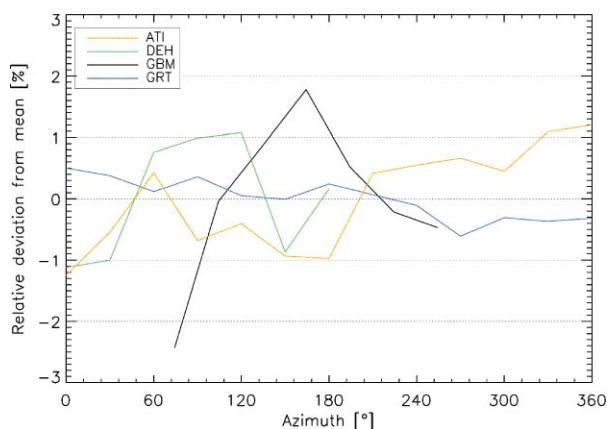


Fig. 7 Relative deviation of spectral zenith radiance at 340 nm and at azimuth angles between 0° and 360°. The measurements of each instrument are normalized to their average and corrected for changes in radiance during the period of measurements. The deviations are within the precision of the instruments and do not indicate any dependence on polarization.

Due to hardware limitations of the tracking devices of DEH (green line) and GBM (black line), it was not possible to measure the polarization by turning the devices by 360° with these instruments. Instead, polarization was measured for only 180° and it was assumed to be symmetrical.

Spectral sky radiance measurements from Thessaloniki

Spectral measurements of zenith sky radiance were conducted in Thessaloniki during a partly cloudy day on 14 July 2006 and during two cloud free days on 23 July 2006 and 24 July 2006. Results of the GRT instrument are plotted in Fig. 8. All spectra were of the zenith, therefore their shape remains similar compared to the shapes of the spectra of Fig. 3 which were measured at different directions (see Table 3).

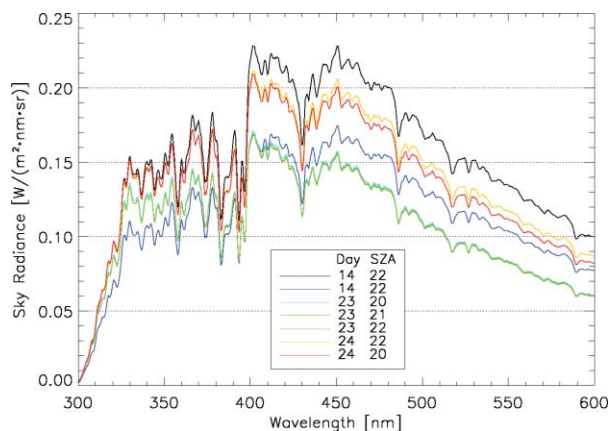


Fig. 8 Spectral zenith sky radiance spectra measured by means of the GRT instrument in Thessaloniki on different days. Compared to the measurements in Izaña the spectral sky radiance measured in Thessaloniki is almost twice as high at its maximum between 400–410 nm.

There are two major reasons why the spectral sky radiance measured in Thessaloniki is for some days twice as high as in Izaña. Firstly, Thessaloniki is located at sea level whereas the Izaña observatory is positioned at an altitude of ~2.4 km. The mean surface pressure at the Izaña station during the measurements was 770 hPa whereas it was 1014 hPa at Thessaloniki. This additional mass of air leads to increased scattering. Secondly, the air above Thessaloniki has larger aerosol loading compared to Izaña. The difference in aerosol optical depth (AOD) at 340 nm between the two locations is more than 0.34.

For the cloud free days (23 and 24 July) the results of successive measurements are close to each other. But on the partly cloudy day (14 July) measurements performed within two minutes differ by about 35%. This is due to a cloud being partially in the field of view of the radiance input optics during the 11:30 UTC (black line) measurement, and then being absent for the 11:32 UTC (blue line) measurement. Due to reflections of the direct beam at the cloud edges the radiance was enhanced due to Mie scattering within the cloud. This scattering process causes a homogeneous wavelength distribution of scattered radiation which is seen by taking the ratio of the two spectra. The enhancement of radiation due to clouds for irradiance has been already described.³⁴

Fig. 9 shows the result of the comparison of zenith sky radiance measurements performed on 14 July 2006 at 11:30 UTC (SZA ~23°; upper panel) and 24 July 2006 at 10:00 UTC (SZA ~21°; lower panel) for ATI, GRT, and USB to DEH.

On 14 July the ratio of ATI to DEH is not constant over the entire wavelength range. There are two wavelength ranges where the increase of the ratio is sudden, 360 to 370 nm and 420 to 430 nm.

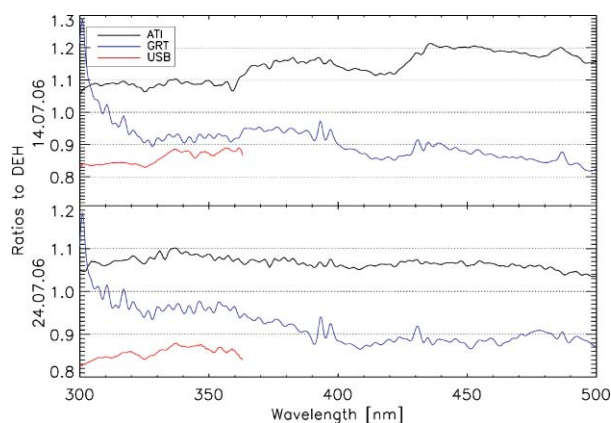


Fig. 9 Comparison of the spectral zenith sky radiance measurements during the campaign in Thessaloniki on 14th and 24th of July, 2006 at 11:30 UTC and 10:00 UTC, respectively, with the measurements of DEH.

For the GRT/DEH ratio the regions with steep increases remain the same as for the ATI/DEH ratio but here the increase is not as pronounced. Since the bounds of the ratio appear in two independent ratios at the same wavelength positions the measurement of DEH seems to be the cause.

The ratio USB/DEH shows an increase with increasing wavelength. But since the ratio stops at 364 nm as the USB-Brewer is not able to measure radiation of longer wavelengths, it is not possible to see if this ratio would also have exhibited steep increases.

The lower panel of Fig. 9 shows ratios of DEH measurement to the measurements of other groups on 24 July at 10:00 UTC. The ratio of ATI to DEH is relatively stable for the entire wavelength range between 1.05 and 1.1.

In contrast, the ratio GRT to DEH is not constant for long wavelength intervals. The best agreement with a deviation of 5% can be found in the shortwave range up to 370 nm.

The pattern of USB to DEH comparison is very similar to the ratio of ATI/DEH at the same wavelength range.

The sudden increases of the ratio as seen in the upper panel are not visible for the ratios of measurements from 24 July.

Fig. 10 shows ratios of spectral zenith sky radiance measurements of ATI, DEH, GRT, and USB to the UVSPEC RT model calculations on 14 July at 11:30 UTC (upper panel) and

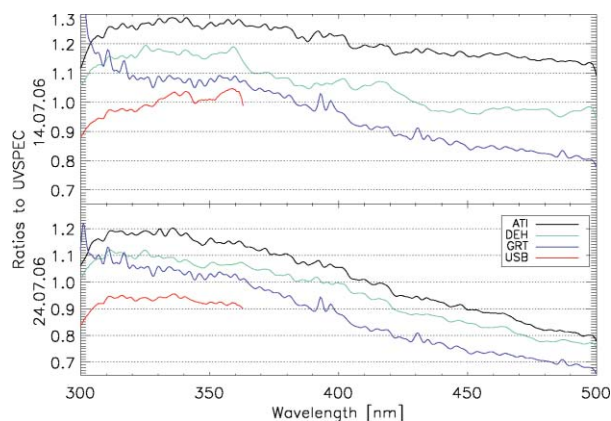


Fig. 10 Comparison of the spectral zenith sky radiance measurements during the campaign in Thessaloniki on 14th and 24th of July, 2006 at 11:30 UTC and 10:00 UTC, respectively, with RT model calculations.

on 24 July at 10:00 UTC (lower panel). The input parameters for the RT model are listed in Table 2. To diminish the error arising from choosing a constant SZA from the beginning of each measurement, the SZA has been calculated for each wavelength separately since the measurements were synchronized.

The SZA was around 23° during the measurements at 11:30 UTC on 14 July. The highest deviation to RT calculations is seen for ATI. The ratio is always above 1.1 and especially in the UV range the deviation from the RT calculation is higher than 20%.

The ratio DEH/UVSPEC decreases continuously from 1.1 to 0.97. A slight wavy structure for the entire wavelength range can be seen which would explain similar behaviour of the ratios in Fig. 8 on 14 July because all measurements were normalised to the DEH measurement.

The ratio of the measurement of GRT to the UVSPEC model calculation also constantly decreases over the entire wavelength range.

The best agreement to the RT calculations was from the measurement performed by USB. Apart from the first 10 nm the deviation is $\pm 5\%$.

At the beginning of all ratios a significant increase can be seen which leads to the assumption that the measured value for ozone concentration might not be in accordance with the real ozone concentration in the atmosphere. In contrast, the ratio of GRT decreases between 300 and 310 nm which indicates a high level of stray light within the single monochromator instrument.

The SZA was around 21° during the measurements at 10:00 UTC on 24 July. It can be seen that the most noticeable feature of all the ratios is that they all decrease at longer wavelengths.

ATI decreases from 1.2 to 0.9, DEH from 1.1 to 0.77, and GRT decreases from 1.1 to 0.7. The difference between all three ratios remains almost constant from 360 to 500 nm.

Only the ratio USB/UVSPEC remains almost constant at 0.95 between 310 and 360 nm with a slight decrease for wavelength longer than 340 nm.

The results show that with the AOD and single scattering albedo (SSA) measured by both the Cimel sun photometer (at 440 nm) and the shadowband radiometer (340 nm) the zenith radiances agree very well with USB. However the measured SSA was rather low. A higher SSA would bring the modelled radiances towards the DEH-ATI measurements. So although the RT model cannot be used to support the calibration of any individual instrument, it provides further evidence that the actual values lie in the range covered by the ground instruments.

Spectral radiance calibration comparison in Innsbruck

The calibration setup of the GRT group consists of a calibrated halogen lamp with an irradiance certificate E_{GRT} that is mounted at a distance of 50 cm to a reflectance plate (see paragraph GRT for detailed description). The reflectance plate is perpendicularly illuminated. The spectral reflectivity R of the plate, which is referring to hemispherical reflectance, is between 97% and 99% for wavelengths from 250 to 900 nm. The reflectance plate is assumed to be a Lambertian reflector that is radiating the incident light in a solid angle of π . Therefore the radiance certificate of the reflectance plate L_{GRT} is given by eqn (1).

Because the lamp is positioned perpendicularly to the reflectance plate it is difficult to arrange the input optics likewise.

So the radiance input optics is positioned near the lamp, thereby looking at the illuminated reflectance plate at a small viewing angle (VA).

By contrast the calibration setup of the ATI group is based on measuring the output light of a calibrated integrating sphere (see paragraph ATI for detailed description). Both calibration setups are completely independent of each other.

First the lamp certificate E_{GRT} measured in Greece with the GRT instrument was checked for consistency by measuring global irradiance E_{ATI} with the calibrated input optics of ATI at a distance of 50 cm to the lamp L_{G} . An offset of +2% for wavelengths below 500 nm between both lamp certificates E_{GRT} and E_{ATI} was found, which is well within the uncertainties of the primary lamp certificates of both groups. The same offset is found of course by comparing L_{GRT} and L_{ATI} (eqn (1)), see Fig. 11.

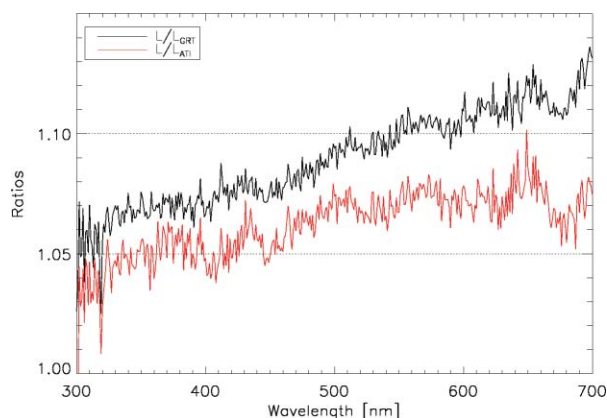


Fig. 11 Comparison of two independent radiance calibration setups using on the one hand an integrating sphere and on the other hand an illuminated reflectance plate (for details see text).

Then both calibration setups were used to calibrate the radiance input optics of both groups. Great care was taken to avoid stray light reflections while calibrating with the reflectance plate. The calibration of the radiance input optics with the integrating sphere is very insensitive to stray light but the whole FOV of the input optics must be illuminated by the light exiting the sphere in order to obtain reliable results. So the input optics has to be positioned at a short distance (about 10 cm) to the output port of the sphere.

In order to compare the two independent calibration methods first the radiance input optic of ATI was calibrated with the integrating sphere. Then the radiance L of the illuminated reflectance plate was measured with the ATI optic looking at a viewing angle of 12.5° on the reflectance plate. In Fig. 11 the ratios of the radiance L of the plate to the certificates of the plate L_{GRT} and L_{ATI} are shown, thereby directly comparing both calibration methods. The two curves show the effect of changing the plate certificate due to the measurement of the GRT primary calibration lamp by ATI (E_{GRT} and E_{ATI} , see discussion above).

In conclusion the maximum difference of 33% found between measurements of both groups in Thessaloniki can not be explained by the results obtained in Innsbruck where a general agreement of the order of <7% was found.

Discussion

The major part of the uncertainty regarding spectral sky radiance measurements originates from the calibration procedure, but a significant cause of deviations in the measurements is still unknown. The difference between measurements performed by different groups is as high as 33% and the deviation to model results can also exceed 30% for some wavelengths. In contrast the difference between measurements of spectral global irradiance during the same Izaña campaign, where the presented spectral sky radiance was measured, was at most 8%.

For global irradiance measurements there is a standardized calibration method and the input optics are of comparable quality. The calibration method implies the usage of a secondary calibration standard (*i.e.* 1000 W FEL lamp) in front of the diffuser used for global irradiance measurements.

For absolute radiometric calibration of spectral radiance three different methods are used in this publication:

1. Calibrating the irradiance port and converting to a radiance calibration using the instrument's field of view;
2. Using a diffuser plate to diffuse the direct beam of a calibration lamp;
3. Using an integrating sphere with a known spectral radiation output.

Using method 1, the FOV of the input optics has to be considered. A lamp needs to be a point source, for calibration, an assumption that breaks down if the input optics are too close. This means that the lamp does not illuminate the entire FOV of the input optics which may lead to some errors because in case of an inhomogeneous optical fibre bundle the entrance slit of the monochromator is not evenly illuminated. But the advantages of this method are that it requires less laboratory equipment and the noise level in the calibration is lower due to the high lamp output.

Diffuse reflected radiation from a reflectance plate (method 2) or an integrating sphere (method 3) illuminates the entire FOV and consequently the interior of the used input optics. A disadvantage for method 2 is the potential error source of scattered light from the lamp reaching the diffuser.

In general, the maximum deviation of absolute calibration compared to the values of DEH seems higher for ATI (~8%) and GBM (~5%), and lower for GRT (~15%) and USB (~14%) at 360 nm. Table 4 lists the maximum difference between DEH and the other participant of both measurement campaigns at 360 nm.

In Izaña ATI was 3% higher than DEH. Between the campaigns in Izaña and Thessaloniki ATI changed its calibration procedure from a reflectance plate to an integrating sphere which could explain the increase of the difference to DEH by 4 to 5%. If one considers that the data of DEH should be 2% higher due to the $R(0^\circ/45^\circ, \lambda)$ vs. $R(8^\circ/h, \lambda)$ calibration setup (see calibration

Table 4 Difference in percentage of absolute radiance measurements of ATI, GBM, GRT, and USB to measurements of DEH at 360nm

	Izaña (06.06.2005)	Thessaloniki (14.07.2006)	Thessaloniki (24.07.2006)
ATI	+3%	+8%	+7%
GBM	+5%	N/A	N/A
GRT	+15%	-8%	-5%
USB	N/A	-12%	-14%

description of DEH in the “Instruments and methods” section), the deviation between ATI and DEH is below the measurement uncertainty.

The reason for the discrepancy of GRT between the Izaña (+15%) and Thessaloniki (−8% and −5%) campaigns compared to the reference instrument of DEH is that the CCD instrument was delivered in March 2005. Therefore at the Izaña campaign it was not yet fully characterized and its operation had not been optimized. Post processing of the data set revealed a difference of 15% to the reference instrument which is a combined result of errors arising from the calibration and measuring processes. At the campaign in Thessaloniki a number of calibration and measurement issues were resolved resulting in reduction of this difference down to 5%. The 3% day-to-day variability is considered to be within the measuring uncertainty of the instrument.³⁵

During the Thessaloniki campaign the USB direct sun irradiance measurements agree very well ($\pm 3\%$) with those performed by ATI. Furthermore, the USB direct sun irradiance measurements agree very well with those from the Cimel Aeronet sun photometer, both before and after the Thessaloniki campaign. The USB direct irradiance is calibrated using methods 2 and 3, but then using the FOV to go from radiance calibration to irradiance calibration (basically the inverse of method 1). Since the USB direct irradiance measurements agree well during the Thessaloniki campaign with ATI and Aeronet, this means that either both the radiance calibration and the field of view are correct or that the radiance calibration and the field of view have the same errors of the opposite sign. So there is an unexplained discrepancy of at least 10%.

The FOV of the entrance optic should not influence the determination of spectral sky radiance for a cloudless sky. During the comparisons in Izaña and Thessaloniki, spectral sky radiance measurements performed with input optics with different FOV did not show any common bias. For example, the measurements of ATI and USB which both use a narrow FOV input optics (1.4° and 0.5°, respectively) are higher for ATI and lower for USB compared to DEH, which uses an input optics with a FOV of 4.5°. If there was an influence due to the FOV one would expect that both measurements would have been either higher or lower compared to DEH.

More works needs to be done on this topic to effectively explain the uncertainties arising from different calibration procedures and input optics with different FOV.

Conclusions

Spectral sky radiance measurements by five scientific groups have been performed at three different locations. The deviation of measured spectral sky radiance varies between 3 and 35% depending on wavelength, location and instrument. While such deviations may be acceptable for some applications, especially if relative values are needed, it is not satisfactory for other applications. Compared to measurements of spectral irradiance the observed deviations are relatively large. It should be emphasized, however, that it took more than a decade of intensive intercomparisons and laboratory characterization until estimated uncertainties and observed deviations of spectral irradiance came into a satisfactory agreement for a larger number of instruments. A similar situation is now expected for spectral radiance measurements. Therefore it is not surprising

that it has not yet been possible to explain differences of up to 35% between ATI and GRT during the measurements conducted in Thessaloniki. While calibration procedures seem to be a large source of uncertainty, there are probably additional significant uncertainties caused by the instrument movement and setup. The range of uncertainties presented by the groups for their calibration setups are state-of-the-art, but need to be improved in future by additional laboratory measurements. In clear sky conditions the various FOVs of the radiance input optics do not seem to have a large influence on the measured radiance. We conclude that the accurate measurement of spectral sky radiance will remain a challenge for a while and we believe that standardised, comparable calibration methods need to be developed for reliable absolute spectral radiance measurements.

Acknowledgements

Part of this study has been conducted in the framework of the EC Integrated Project SCOUT-O3 (contract 505390-GOCE-CT-2004). We would like to thank WMO for providing financial support to groups taking part in the Izaña campaign. Furthermore, we are indebted to the director of the Izaña Observatory, Dr Emilio Cuevas for providing the facilities to host the campaign and to Alberto Redondas for his continuous support during the campaign.

Notes and references

- 1 G. Seckmeyer, A. F. Bais, G. Bernhard, M. Blumthaler, P. Eriksen, R. L. McKenzie, C. Roy and M. Miyauchi, Instruments to Measure Solar Ultraviolet Radiation, Part I: Spectral Instruments, *Tech. Rep.*, 2001, **30**, WOM-GAW.
- 2 C. Dorno, *Studie über Licht und Luft des Hochgebirges*. Vieweg & Sohn, Braunschweig, 1911.
- 3 P. Bener, Der Einfluß der Bewökung auf die Himmelsstrahlung, *Arch. Met. Geoph. Biokl.*, 1963, **B**, **12**, 442–457.
- 4 M. Blumthaler, J. Gröbner, M. Huber and W. Ambach, Measuring spectral and spatial variations of UVA and UVB sky radiance, *J. Geophys. Res.*, 1996, **23**(5), 547–550.
- 5 P. J. Ricchiuzzi, A. Payton, C. Gautier, eds., The Effect of Surface Albedo Heterogeneity on Sky Radiance, *Tenth ARM Science Team Meeting Proceedings*, 2000, San Antonio, Texas.
- 6 M. Huber, M. Blumthaler, J. Schreder, B. Schallhart and J. Lenoble, Effect of inhomogeneous surface albedo on diffuse UV sky radiance at a high-altitude site, *J. Geophys. Res.*, 2004, 109.
- 7 S. Wuttke, *Radiation conditions in an Antarctic environment*, Ph.D. thesis, 2004, Universität HannoverGermany, <http://hdl.handle.net/10013/epic.24495>.
- 8 S. Wuttke and G. Seckmeyer, Spectral Radiance and Sky Luminance in Antarctica: A Case Study, *Theor. Appl. Climatol.*, 2006, **85**, 131–148.
- 9 S. Wuttke, G. Seckmeyer, G. Bernhard, J. Ehrhamjian, R. McKenzie, P. Johnston and M. O’Neil, New spectroradiometers complying with the NDSC standards, *J. Atmos. Oceanic Technol.*, 2006, **23**(2), 241–251.
- 10 G. Seckmeyer, Spektralradiometer für die ökologische Pflanzenforschung, *Licht*, 1989, **41**, 7–8.
- 11 G. Meister, P. Abel, *et al.*, The first SIMBIOS radiometric intercomparison (SIMRIC-1), *April-September 2001 Report NASA/TM-2002*, 2002, Goddard Space Flight Center, Greenbelt, Maryland, USA.
- 12 G. Bernhard and G. Seckmeyer, Uncertainty of measurements of spectral solar UV irradiance, *J. Geophys. Res.*, 1999, **104**(D12), 14321–14345.
- 13 B. C. Johnson, S. S. Bruce, *et al.*, The Fourth SeaWiFS Intercalibration Round-Robin Experiment (SIRREX-4), May 1995, *NASA Tech. Memo. 104566*, 1996, 37, NASA Goddard Space Flight Center, Greenbelt, Maryland.
- 14 L. M. Hanssen, and K. A. Snail, in *Handbook of Vibrational Spectroscopy*, 2001, ed. by J. Chalmers, and P. Griffiths, p. 1175–1191.

- 15 R. R. Cordero, G. Seckmeyer, D. Pissulla, L. DaSilva and F. Labbe, Uncertainty evaluation of spectral UV irradiance measurements, *Measurement Science & Technology*, 2008, **19**(045104), 1–15.
- 16 R. R. Cordero, G. Seckmeyer, D. Pissulla and F. Labbe, Uncertainty of experimental integrals: application to the UV index calculation, *Metrologia*, 2008, **45**, 1–10.
- 17 A. F. Bais, B. G. Gardiner, H. Slaper, M. Blumthaler, G. Bernhard, R. L. McKenzie, A. R. Webb, G. Seckmeyer, B. Kjeldstad, T. Koskela, P. Kirsch, J. Gröbner, J. B. Kerr, S. Kazadzis, K. Leszczynski, D. Wardle, C. Brogniez, W. Josefsson, D. Gillotay, H. Reinen, P. Weihs, T. Svenoe, P. Eriksen, F. Kuik and A. Redondas, The SUSPEN intercomparison of ultraviolet spectroradiometers, *J. Geophys Res*, 2001, **106**, 12509–12526.
- 18 A. R. Webb, A. F. Bais, M. Blumthaler, G.-P. Gobbi, A. Kylling, R. Schmitt, S. Thiel, F. Barnaba, T. Danielsen, W. Junkermann, A. Kazantzidis, P. Kelly, R. Kift, G. L. Liberti, M. Misslbeck, B. Schallhart, J. Schreder and C. Topaloglou, Measuring spectral actinic flux and irradiance: Experimental results from the actinic flux determination from measurements of irradiance (ADMIRA) project, *J. Atmos. Oceanic Technol.*, 2002, **19**, 1049–1062.
- 19 A. F. Bais, M. Blumthaler, A. Webb, G. Seckmeyer, S. Thiel, S. Kazadzis, A. Redondas, R. Kift, N. Kouremeti, B. Schallhart, R. Schmitt, D. Pissulla, J. P. Diaz, O. Garcia, A. M. Diaz, Rodriguez, A. Smedley, Intercomparison of solar UV direct irradiance spectral measurements at Izaña in June 2005, in *Ultraviolet Ground- and Space-based Measurements, Models, and Effects V*. Edited by Bernhard, Germar; Slusser, R. James, Jay R. Herman, Wei. Gao, *Proceedings of the SPIE*, Volume 5886, 2005, 73–82.
- 20 F. E. Nicodemus, J. C. Richmond, J. J. Hsia, I. W. Ginsberg, and T. Limperis, Geometrical considerations and nomenclature for reflectance, in *Final Report National Bureau of Standards, Washington, DC.*, 1977, Inst. for Basic Standards, Editors K. F. Galloway, and P. Roitman.
- 21 S. Sandmeier, C. Müller, B. Hosgood and G. Andreoli, Sensitivity analysis and quality assessment of laboratory BRDF data, *Remote Sensing of Environment*, 1998, **64**(2), 176–191.
- 22 J. B. Kerr, C. T. McElroy, D. I. Wardle, R. A. Olafson, and W. F. J. Evans, The automated Brewer spectrophotometer, in: *Atmospheric ozone. – Proceedings of the Quadrennial Ozone Symposium*, 1985, C. S. Zerefos, and A. Ghazi, eds. Reidel, Boston, Mass., 396–401.
- 23 A. Cede, J. Herman, A. Richter, N. Krotkov and J. Burrows, Measurements of nitrogen dioxide total column amounts using a Brewer double spectrometer in direct Sun mode, *J. Geophys. Res.*, 2006, **111**, D05304, DOI: 10.1029/2005JD006585.
- 24 J. Gröbner, D. I. Wardle, C. T. McElroy and J. B. Kerr, Investigation of the Wavelength Accuracy of Brewer Spectrophotometers, *Appl. Opt.*, 1998, **37**(36), 8352–8360.
- 25 A. Cede, G. Labow, M. Kowalewski, N. Krotkov, and O. Dubovik, Deriving aerosol parameters from absolute UV sky radiance measurements using a Brewer double spectrometer, in *Ultraviolet Ground- and Space-based measurements, Models, and Effects III*, 4–6 August 2003, San Diego, USA, *Proceedings of SPIE* Vol. 5156, 2003, 323–329, SPIE-The International Society for Optical Engineering, J. R. Slusser, J. R. Herman, and W. Gao, Editors.
- 26 A. Cede, G. Labow, M. Kowalewski, and J. Herman, The effect of polarization sensitivity of Brewer spectrometers on Direct Sun measurements, in *Ultraviolet Ground- and Space-based measurements, Models, and Effects IV*, 5–6 August 2004, Denver, USA, *Proceedings of SPIE* Vol. 5545 2004, 131–137, SPIE-The International Society for Optical Engineering, J. R. Slusser, J. R. Herman, W. Gao, and G. Bernhard, Editors.
- 27 A. Cede, S. Kazadzis, M. Kowalewski, A. Bais, N. Kouremeti, M. Blumthaler and J. Herman, Correction of direct irradiance measurements of Brewer spectrophotometers due to the effect of internal polarization, *Geophys. Res. Lett.*, 2006, **33**(2), L02806, DOI: 10.1029/2005GL024860.
- 28 H. W. Yoon, J. E. Proctor and C. E. Gibson, FASCAL 2: a new NIST facility for the calibration of the spectral irradiance of sources, *Metrologia*, 2003, **40**, S30–S34.
- 29 G. T. Georgiev, and J. J. Butler, Long-term comparison of spectralon BRDF measurements in the ultraviolet, in *Earth Observing Systems IX*, 5–6 August 2004, Denver, USA, *Proceedings of SPIE* Vol. 5542 2004, Pages 323–333, SPIE-The International Society for Optical Engineering, W. L. Barnes, and J. J. Butler, Editors.
- 30 S. Janz, E. Hilsenrath, J. Butler, D. F. Heath and R. P. Cebula, Uncertainties in radiance calibrations of backscatter ultraviolet (BUV) instruments, *Metrologia*, 1995, **32**(6), 637–641.
- 31 H. Slaper, H. A. Reinen, M. Blumthaler, M. Huber and F. Kuik, Comparing ground-level spectrally resolved solar UV measurements using various instruments: A technique resolving effects of wavelength shift and slit width, *Geophys. Res. Lett.*, 1995, **22**, 2721–2724.
- 32 B. Mayer and A. Kylling, Technical note: The libRadtran software package for radiative transfer calculations – description and examples of use, *Atmos. Chem. Phys.*, 2005, **5**, 1855–1877.
- 33 B. N. Holben and T. I. Eck, *et al.*, AERONET-A Federated Instrument Network and Data Archive for Aerosol Characterization, *Remote Sensing of Environment*, 1998, **66**, 1–16.
- 34 G. Seckmeyer, B. Mayer, R. Erb and G. Bernhard, UV-B in Germany higher in 1993 than in 1992, *Geophys. Res. Lett.*, 1994, **21**, 577–580.
- 35 N. Kouremeti, A. F. Bais, S. Kazadzis, M. Blumthaler and R. Schmitt, Charge-coupled device spectrograph for direct solar irradiance and sky radiance measurements, *Appl. Opt.*, 2008, **47**, 1594–1607.